IEICE TRANS. COMMUN., VOL.E90–B, NO.10 OCTOBER 2007

PAPER

Pre- and Post-Equalization and Frequency Diversity Combining Methods for Block Transmission with Cyclic Prefix*

Yuki YOSHIDA[†a)], *Student Member*, Kazunori HAYASHI[†], *and* Hideaki SAKAI[†], *Members*

SUMMARY This paper proposes low-complexity pre- and post-frequency domain equalization and frequency diversity combining methods for block transmission schemes with cyclic prefix. In the proposed methods, the equalization and diversity combining are performed simultaneously in discrete frequency domain. The weights for the proposed equalizer and combiner are derived based on zero-forcing and minimum-mean-square error criteria. We demonstrate the performance of the proposed methods, including bit-error rate performance and peak-to-average power ratios of the transmitted signal, via computer simulations.

key words: *cyclic prefix, frequency domain equalization, frequency diversity*

1. Introduction

A fundamental problem in high data rate wireless communication systems is the equalization of the received signal distorted by frequency selective fading channels. Frequency domain equalization (FDE) using cyclic prefix (CP) has been drawing much attention due to its simplicity and robustness to such propagation impairment [1] and has been used in many transmission schemes, such as orthogonal frequency division multiplexing (OFDM) [2], discrete multitone (DMT) [3], or single carrier block transmission with cyclic prefix (SC-CP) [4].

When we consider further performance improvement of the FDE systems, one promising strategy is to employ frequency diversity techniques [5]. In this paper, we firstly propose a low-complexity frequency domain equalization and diversity combining method for the FDE systems. It is well known that sampling the received signal at the rate lower than the signal bandwidth (in other words undersampling or decimation for discrete-time signal) causes aliasing. In the proposed method, we utilize the phenomenon as a frequency diversity combining method and show that the idea is efficiently adopted to the FDE systems by employing oversampling and decimation. Furthermore, it is also shown that, the equalizer and diversity combiner can be realized by an one-tap discrete frequency domain processing (namely, frequency domain equalizer and diversity combiner, FDE/DC). We derive the optimum FDE/DC weights based on both the zero-forcing (ZF) and the minimum mean-square-error (MMSE) criteria. It should be noted that, in general, oversampling at the receiver causes colored noise problem due to the receiving (Rx) filter. In such cases, a linear equalizer and combiner based on the MMSE criterion can not be realized by the configuration of the proposed FDE/DC. Thus, we also derive the linear MMSE equalizer and combiner without assuming any configuration for comparison purpose. Moreover, we propose a novel pre-frequency domain equalization and diversity combining method for the FDE systems. Although the transmitter has to have access to channel state information (CSI), the receiver of the proposed pre-equalization and diversity combining system becomes extremely simple, while it can achieve diversity gain. Finally, we demonstrate the performance of the proposed methods, including the bit-error rate (BER) performance and the peak-to-average ratio (PAPR) of the transmitted signal, via computer simulations.

This paper is arranged as follows. In Sect. 2, we introduce the proposed equalization and diversity combining method for the SC-CP scheme. The proposed pre-equalization and diversity combining method is discussed in Sect. 3. In Sect. 4, we adopt the proposed methods to the OFDM scheme. The results of the computer simulations and conclusions appear in Sect. 5 and Sect. 6.

The notation used in this paper follows the usual convention — bold capital letters are used to denote column vectors or matrices and $(\cdot)^*$, $(\cdot)^T$, and $(\cdot)^H$, are complex conjugate, transpose, and Hermitian transpose of $(\cdot)$ respectively. An $M \times M$ identity matrix is denoted by $\mathbf{I}_M$ and $\mathbf{0}_{M\times N}$ is an all-zero matrix of size $M \times N$. We also use E[·] to denote ensemble average, tr{·} for trace, and $\|\cdot\|^2$ for Euclidean norm.

2. Proposed Equalization and Diversity Combining Method for SC-CP Scheme

2.1 System Description

Figure 1 shows the configuration of the SC-CP scheme with the proposed equalization and frequency diversity combining method. In the figure, M denotes the block size and N is the CP length. In order to generate frequency diversity signals, the information-bearing signals after the CP insertion are modulated by an impulse train $\sum_n \delta(t - nT_s)$ of the symbol rate $1/T_s$ and filtered by the transmitting (Tx) filter whose pulse shape $f_P(t)$ has $P(\geq 1)$ times larger passband width than the symbol rate. Therefore, in the proposed system, due to the CP insertion and the extended

Manuscript received April 6, 2006.
Manuscript revised October 31, 2006.

[†]The authors are with the Graduate School of Informatics, Kyoto University, Kyoto-shi, 606-8501 Japan.

*A part of this work was already presented in [11].

a) E-mail: yyoshida@sys.i.kyoto-u.ac.jp

DOI: 10.1093/ietcom/e90–b.10.2874

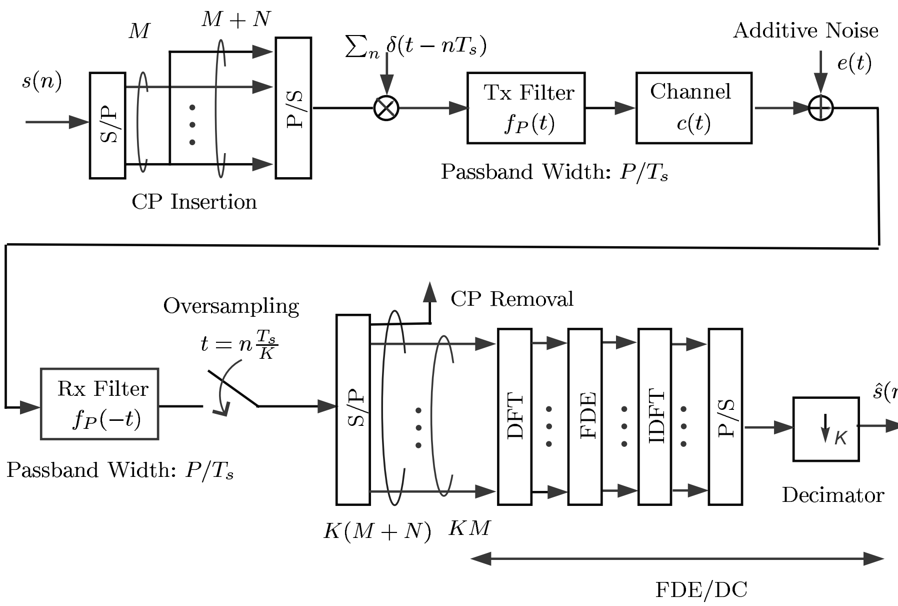

Fig. 1 The configuration of the SC-CP scheme with the FDE/DC.

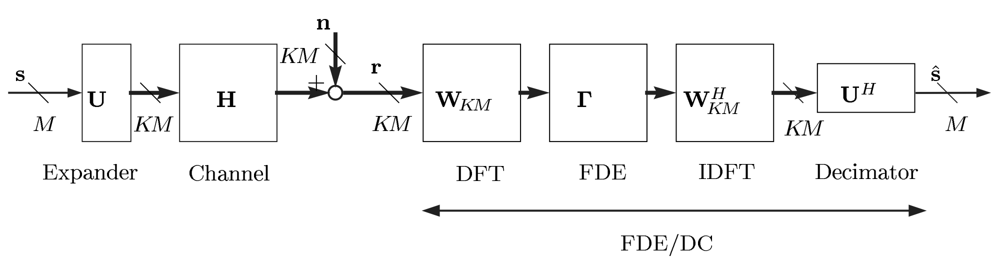

Fig. 2 The block diagram of SC-CP scheme with the FDE/DC.

pass band width, the total frequency efficiency is reduced to $M/P(M+N)$.

At the receiver, to observe the whole transmitted signal spectrum, the received signals are sampled at the rate K times higher than the symbol rate, where K is an integer and satisfies $K \geq P$. KM samples after the CP removal are then processed by the FDE/DC. The FDE/DC utilizes KM-point discrete Fourier transform (DFT) and the decimator which is the operation of picking up every K-th symbols.

In the proposed system, the transmitted signal spectrum has multiple copies of its original spectrum. Since the FDE equalize whole copies distorted by the channel, we can easily realize the frequency diversity by combining the copies through aliasing due to the decimator.

Strictly speaking, the weights of the FDE is chosen for not only the equalization but also the weighting for diversity combining. Thus we call it the FDE/DC weights. It should be also noted that the proposed system configuration covers the SC-CP scheme without the frequency diversity when $P = 1$. Especially, when $K > 2$ while $P = 1$, the proposed system results in the same configuration as the SC-CP system with the fractionally spaced equalizer (FSE) [6], [7]. In [6], authors have been derived the ZF weights for the FSE in the case of $K = 2$. In this section, we will consider ZF based FDE/DC weights in the case of $K \geq 2$, and also derive the MMSE based weights.

The block diagram of the proposed system is shown in Fig. 2. In the figure, $\mathbf{s}$ denotes an $M \times 1$ vector of the information-bearing signal block, where we drop the block index for simplicity, $\mathbf{r}$ is a $KM \times 1$ vector of the corresponding received signals after the oversampling, and $\hat{\mathbf{s}}$ is an $M \times 1$ vector of the equalizer output. The oversampling at the receiver can be expressed as the expander operation, inserting $K-1$ zeros between two neighboring symbols, at the transmitter in the discrete time signal model [9]. In the block transmission settings, the expander can be represented by a $KM \times M$ matrix $\mathbf{U}$, whose Km-th row is equal to the m-th row of $\mathbf{I}_M$ and the other rows are zero. For example, if $K = 2$ and $M = 3$,

$$\mathbf{U} = \begin{bmatrix} 1 & 0 & 0 \\ 0 & 0 & 0 \\ 0 & 1 & 0 \\ 0 & 0 & 0 \\ 0 & 0 & 1 \\ 0 & 0 & 0 \end{bmatrix}. \tag{1}$$

Also, the decimator is represented by $\mathbf{U}^H$. In our approach, we assume that the length of the CP is long enough to support the channel and, thanks to the CP, the channel can be expressed by a $KM \times KM$ circulant matrix $\mathbf{H}$, where the first (i.e., the 0-th) column is given by $\mathbf{h} = [h(0), h(1), \cdots, h(L), 0, \cdots, 0]^T$. Here, $h(n)$ is the channel coefficients including the Tx and Rx filters and L is the order of the whole channel. $\mathbf{W}_M$ denotes the M-point DFT matrix, where the (m, n) element $(m, n = 0, 1, \cdots, M)$ is given by

$$\mathbf{W}_M(m, n) = \frac{1}{\sqrt{M}} e^{-j \cdot 2\pi mn/M}, \tag{2}$$

and $\mathbf{W}_M^H$ is the M-point inverse discrete Fourier transform (IDFT) matrix. The circulant matrix $\mathbf{H}$ can be diagonalized by pre- and post-multiplication with KM-point DFT and IDFT matrices [8], i.e., $\mathbf{H} = \mathbf{W}_{KM}^H \mathbf{\Lambda} \mathbf{W}_{KM}$, where $\mathbf{\Lambda} = \mathrm{diag}\{\lambda(0), \lambda(1), \cdots, \lambda(KM-1)\}$ is a $KM \times KM$ diagonal matrix whose diagonal elements are the KM-point DFT of $\mathbf{h}$. Thus $\mathbf{r}$ can be written as

$$\mathbf{r} = \mathbf{W}_{KM}^H \mathbf{\Lambda} \mathbf{W}_{KM} \mathbf{U} \mathbf{s} + \mathbf{n}, \tag{3}$$

where $\mathbf{n}$ is a $KM \times 1$ noise vector. It should be noted that, when the oversampling factor K is greater than the expansion rate P, the noise is no more white due to the Rx filter. The output $\hat{\mathbf{s}}$ is given by

$$\hat{\mathbf{s}} = \mathbf{U}^H \mathbf{W}_{KM}^H \mathbf{\Gamma} \mathbf{W}_{KM} \mathbf{r}, \tag{4}$$

where $\mathbf{\Gamma} = \mathrm{diag}\{\gamma(0), \gamma(1), \cdots, \gamma(KM-1)\}$ is a $KM \times KM$ diagonal matrix of the FDE/DC weights.

2.2 Simplified Configuration for the FDE/DC

Here, we simplify the block diagram of the FDE/DC. Since post-multiplication with $\mathbf{U}$ is the operation to extract every K-th columns of the multiplied matrix, the (m, n) element of $\tilde{\mathbf{U}} := \mathbf{W}_{KM} \mathbf{U}$ is given by

$$\begin{aligned} \tilde{\mathbf{U}}(m, n) &= \frac{1}{\sqrt{KM}} e^{-j \cdot 2\pi \cdot m(Kn+1-1)/KM}, \\ &= \frac{1}{\sqrt{K}} \cdot \frac{1}{\sqrt{M}} e^{-j \cdot 2\pi \cdot mn/M}, \\ &= \frac{1}{\sqrt{K}} \cdot \mathbf{W}_M(l, n), \end{aligned} \tag{5}$$

where $l := m \pmod{M}$, $m = 0, 1, \cdots, KM-1$, and $n = 0, 1, \cdots, M-1$. Thus, we have

$$\tilde{\mathbf{U}} = \frac{1}{\sqrt{K}} \begin{bmatrix} \mathbf{W}_M \\ \vdots \\ \mathbf{W}_M \end{bmatrix} = \frac{1}{\sqrt{K}} \begin{bmatrix} \mathbf{I}_M \\ \vdots \\ \mathbf{I}_M \end{bmatrix} \mathbf{W}_M. \tag{6}$$

From (4) and (6), we can rewrite the output $\hat{\mathbf{s}}$ as

$$\hat{\mathbf{s}} = \frac{1}{\sqrt{K}} \mathbf{W}_M^H \begin{bmatrix} \mathbf{\Gamma}_0 & \mathbf{\Gamma}_1 & \ldots & \mathbf{\Gamma}_{K-1} \end{bmatrix} \mathbf{W}_{KM} \mathbf{r}, \tag{7}$$

where $\mathbf{\Gamma}_k = \mathrm{diag}\{\gamma(kM), \cdots, \gamma((k+1)M-1)\}$ $(k = 0, 1, \cdots, K-1)$ is an $M \times M$ submatrix of $\mathbf{\Gamma}$. Therefore, the configuration of the FDE/DC can be redrawn as in Fig. 3. Defining $M \times M$ submatrices $\mathbf{\Lambda}_k = \mathrm{diag}\{\lambda(kM), \cdots, \lambda((k+1)M-1)\}$ $(k = 0, 1, \cdots, K-1)$, we have

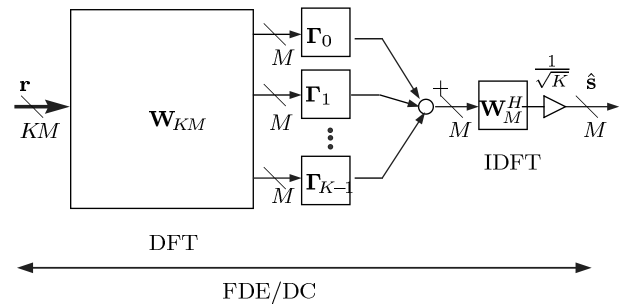

Fig. 3 The simplified block diagram of the FDE/DC.

$$\begin{aligned} \hat{\mathbf{s}} =& \frac{1}{K} \mathbf{W}_M^H \begin{bmatrix} \mathbf{\Gamma}_0 \mathbf{\Lambda}_0 + & \ldots & + \mathbf{\Gamma}_{K-1} \mathbf{\Lambda}_{K-1} \end{bmatrix} \mathbf{W}_{KM} \mathbf{s} \\ &+ \frac{1}{\sqrt{K}} \mathbf{W}_M^H \begin{bmatrix} \mathbf{\Gamma}_0 & \ldots & \mathbf{\Gamma}_{K-1} \end{bmatrix} \mathbf{W}_{KM} \mathbf{n}. \end{aligned} \tag{8}$$

In the conventional SC-CP system [1], if we assume the order of complex multiplication for M-point FFT as $O(M \log M)$ [10], the computational complexity for the FDE is $2O(M \log M) + O(M)$, i.e., M-point FFT and IFFT, and M weight multiplications. On the other hand, from Fig. 3, the FDE/DC requires K times larger size FFT than that of conventional FDE and use the KM weights and its complexity is represented by $O(KM \log(KM)) + O(M \log(M)) + O(KM)$. Since $K \ll M$ in general, the increase in computation complexity by using the FDE/DC can be given by $O((K-1)M \log(KM))$.

2.3 Weights of FDE/DC

2.3.1 ZF-FDE/DC Weights

First, we derive the ZF criterion-based weights of the FDE/DC with the similar way as in [6]. Here, thanks to the succsessful fomulation (6), we can extend the idea to the cases $K > 2$.

The ZF condition is given by $\hat{\mathbf{s}}(n) = \mathbf{s}(n)$ in the absence of noise, i.e.,

$$\begin{aligned} \hat{\mathbf{s}} &= \frac{1}{K} \mathbf{W}_M^H \begin{bmatrix} \mathbf{\Gamma}_0 \mathbf{\Lambda}_0 + & \ldots & + \mathbf{\Gamma}_{K-1} \mathbf{\Lambda}_{K-1} \end{bmatrix} \mathbf{W}_{KM} \mathbf{s}, \\ &\Longleftrightarrow \mathbf{\Gamma}_0 \mathbf{\Lambda}_0 + \cdots + \mathbf{\Gamma}_{K-1} 3g \mathbf{\Lambda}_{K-1} = K \mathbf{I}_M, \\ &\Longleftrightarrow \boldsymbol{\nu}_m^H \boldsymbol{\xi}_m = K, \quad (m = 0, 1, \ldots, M-1), \end{aligned} \tag{9}$$

where $K \times 1$ vectors $\boldsymbol{\nu}_m$ and $\boldsymbol{\xi}_m$ are defined as follows:

$$\boldsymbol{\nu}_m = [\gamma^*(m) \; \gamma^*(m+M) \; \cdots \; \gamma^*(m+(K-1)M)]^T, \tag{10}$$

$$\boldsymbol{\xi}_m = [\lambda(m) \; \lambda(m+M) \; \cdots \; \lambda(m+(K-1)M)]^T. \tag{11}$$

When $K \geq 2$, (9) has a certain freedom in the choice of $\boldsymbol{\nu}_m$ as shown in [6]. Hence, we also exploit this freedom to minimize the effect of additive noise at the FDE/DC output, i.e., $\mathrm{E}[\|\mathbf{e}\|^2]$, where

$$\mathbf{e} := \frac{1}{\sqrt{K}}\mathbf{W}_M^H[\boldsymbol{\Gamma}_0 \ldots \boldsymbol{\Gamma}_{K-1}]\mathbf{W}_{KM}\mathbf{n}. \tag{12}$$

Denoting the autocorrelation matrix of $\mathbf{n}$ as $\mathbf{R}$, $\mathrm{E}[\|\mathbf{e}\|^2]$ can be calculated as

$$\begin{aligned}\mathrm{E}[\|\mathbf{e}\|^2] &= \frac{1}{K}\mathrm{tr}\left\{[\boldsymbol{\Gamma}_0 \ldots \boldsymbol{\Gamma}_{K-1}]\tilde{\mathbf{R}}\begin{bmatrix}\boldsymbol{\Gamma}_0^H \\ \vdots \\ \boldsymbol{\Gamma}_{K-1}^H\end{bmatrix}\right\}, \\ &= \frac{1}{K}\sum_{m=0}^{M-1}\boldsymbol{\nu}_m^H\tilde{\mathbf{R}}_m\boldsymbol{\nu}_m, \end{aligned}\tag{13}$$

where $\tilde{\mathbf{R}} := \mathbf{W}_{KM}\mathbf{R}\mathbf{W}_{KM}^H$ and the (i, j) element$(i, j = 0, \cdots, K-1)$ of $\tilde{\mathbf{R}}_m$ is equal to the $(m+iM, m+jM)$ element of $\tilde{\mathbf{R}}$. $\tilde{\mathbf{R}}_m$ is known to the receiver a priori because it can be computed from the frequency response of the Rx filter. By minimizing (13) under the constraint (9), the optimum ZF weights is given by

$$\boldsymbol{\nu}_m = \frac{K\tilde{\mathbf{R}}_m^{-1}\boldsymbol{\xi}_m}{\boldsymbol{\xi}_m^H\tilde{\mathbf{R}}_m^{-1}\boldsymbol{\xi}_m}. \tag{14}$$

2.3.2 MMSE-FDE/DC Weights

Next, we propose the FDE/DC weights based on the MMSE criterion. The mean-squared error (MSE) is given by

$$\begin{aligned}\mathrm{MSE} &:= \mathrm{E}[\|\mathbf{s} - \hat{\mathbf{s}}\|^2] \\ &= \mathrm{E}[\mathrm{tr}\{(\mathbf{s} - \hat{\mathbf{s}})(\mathbf{s} - \hat{\mathbf{s}})^H\}]. \end{aligned}\tag{15}$$

Assuming $\mathrm{E}[\mathbf{s}\mathbf{n}^H] = \mathbf{0}_{M\times KM}$, and $\mathrm{E}[\mathbf{s}\mathbf{s}^H] = \sigma_s^2\mathbf{I}_M$, we have

$$\begin{aligned}\mathrm{MSE} = {}& \sigma_s^2\mathrm{tr}\{\mathbf{I}_M\} - \frac{\sigma_s^2}{K}\mathrm{tr}\{\boldsymbol{\Gamma}_0^H\boldsymbol{\Lambda}_0^H + \ldots + \boldsymbol{\Gamma}_{K-1}^H\boldsymbol{\Lambda}_{K-1}^H\} \\ & - \frac{\sigma_s^2}{K}\mathrm{tr}\{\boldsymbol{\Gamma}_0\boldsymbol{\Lambda}_0 + \ldots + \boldsymbol{\Gamma}_{K-1}\boldsymbol{\Lambda}_{K-1}\} \\ & + \frac{\sigma_s^2}{K^2}\mathrm{tr}\{[\boldsymbol{\Gamma}_0\boldsymbol{\Lambda}_0 + \ldots + \boldsymbol{\Gamma}_{K-1}\boldsymbol{\Lambda}_{K-1}][\boldsymbol{\Gamma}_0^H\boldsymbol{\Lambda}_0^H + \ldots + \boldsymbol{\Gamma}_{K-1}^H\boldsymbol{\Lambda}_{K-1}^H]\} \\ & + \frac{1}{K}\mathrm{tr}\left\{\begin{bmatrix}\boldsymbol{\Gamma}_0 & \ldots & \boldsymbol{\Gamma}_{K-1}\end{bmatrix}\tilde{\mathbf{R}}\begin{bmatrix}\boldsymbol{\Gamma}_0^H \\ \vdots \\ \boldsymbol{\Gamma}_{K-1}^H\end{bmatrix}\right\}. \end{aligned}\tag{16}$$

Using $\boldsymbol{\nu}_m$, $\boldsymbol{\xi}_m$ and $\tilde{\mathbf{R}}_m$, (16) can be represented as

$$\begin{aligned}\mathrm{MSE} = {}& M\sigma_s^2 - \frac{\sigma_s^2}{K}\sum_{m=0}^{M-1}\boldsymbol{\xi}_m^H\boldsymbol{\nu}_m - \frac{\sigma_s^2}{K}\sum_{m=0}^{M-1}\boldsymbol{\xi}_m^T\boldsymbol{\nu}_m^* \\ & + \frac{\sigma_s^2}{K^2}\sum_{m=0}^{M-1}\boldsymbol{\nu}_m^H\boldsymbol{\xi}_m\boldsymbol{\xi}_m^H\boldsymbol{\nu}_m + \frac{1}{K}\sum_{m=0}^{M-1}\boldsymbol{\nu}_m^H\tilde{\mathbf{R}}_m\boldsymbol{\nu}_m. \end{aligned}\tag{17}$$

Since the optimum $\boldsymbol{\nu}_m$, which minimizes (17), satisfies $\partial(\mathrm{MSE})/\partial\boldsymbol{\nu}_m^* = \mathbf{0}_{K\times 1}$, we have

$$-\frac{\sigma_s^2}{K}\boldsymbol{\xi}_m + \frac{\sigma_s^2}{K^2}\boldsymbol{\xi}_m\boldsymbol{\xi}_m^H\boldsymbol{\nu}_m + \frac{1}{K}\tilde{\mathbf{R}}_m\boldsymbol{\nu}_m = \mathbf{0}_{K\times 1}. \tag{18}$$

Assuming $\tilde{\mathbf{R}}_m$ is nonsingular and using matrix inversion lemma [10], the MMSE weights for the FDE/DC are given by

$$\boldsymbol{\nu}_m = \frac{K\tilde{\mathbf{R}}_m^{-1}\boldsymbol{\xi}_m}{\frac{K}{\sigma_s^2} + \boldsymbol{\xi}_m^H\tilde{\mathbf{R}}_m^{-1}\boldsymbol{\xi}_m}. \tag{19}$$

2.4 Linear MMSE Equalizer and Combiner

In the proposed system, when $P \neq K$, the oversampling yields colored noise due to the Rx filter. Hence the FDE/DC including one-tap FDE can not be an optimum linear MMSE equalizer and combiner. Thus we derive the linear MMSE equalizer and combiner for comparison purpose.

Let $M \times KM$ matrix $\mathbf{F}$ denotes the linear equalizer and combiner. The output block $\hat{\mathbf{s}}$ is represented by

$$\hat{\mathbf{s}} = \mathbf{F}\mathbf{U}\mathbf{s} + \mathbf{F}\mathbf{n}. \tag{20}$$

The optimum $\mathbf{F}$ which minimize the MSE, i.e., $\mathrm{E}[\|\mathbf{s} - \hat{\mathbf{s}}\|^2]$ is given by

$$\begin{aligned}\mathbf{F} = {}& \sqrt{K}\,\mathbf{W}_M^H\begin{bmatrix}\boldsymbol{\Lambda}_0^* & \ldots & \boldsymbol{\Lambda}_{K-1}^*\end{bmatrix} \\ & \times\left(\begin{bmatrix}\boldsymbol{\Lambda}_0 \\ \vdots \\ \boldsymbol{\Lambda}_{K-1}\end{bmatrix}\begin{bmatrix}\boldsymbol{\Lambda}_0^* & \ldots & \boldsymbol{\Lambda}_{K-1}^*\end{bmatrix} + \frac{K}{\sigma_s^2}\tilde{\mathbf{R}}\right)^{-1}\mathbf{W}_{KM}. \end{aligned}\tag{21}$$

From (21), we can see that the calculation of $\mathbf{F}$ requires the high computational complexity, because of the inverse matrix.

3. Proposed Pre-Equalization and Diversity Combining Method for SC-CP scheme

3.1 System Description

In this section, we alternatively consider the placing the proposed FDE/DC at the transmitter (namely, pre-FDE/DC) and propose a novel pre-equalization and diversity combining method for SC-CP scheme.

Figure 4 shows the block diagram of the proposed system with the pre-FDE/DC. In the transmitter, the weights for equalization and diversity combining are multiplied before the transmission. All the receiver has to do are filtering with Rx filter, sampling at the information rate and CP removal. The received signal after the CP removal in Fig. 4 is given by,

$$\hat{\mathbf{s}} = \mathbf{U}^H\mathbf{W}_{KM}^H\boldsymbol{\Lambda}\boldsymbol{\Theta}\mathbf{W}_{KM}\mathbf{U}\mathbf{s} + \frac{1}{\rho}\mathbf{U}^H\mathbf{n}, \tag{22}$$

where the $KM \times KM$ diagonal matrix $\boldsymbol{\Theta} = \mathrm{diag}\{\theta(0), \cdots, \theta(KM-1)\}$ represents the pre-FDE/DC weights and the constant ρ is introduced to equate the power of the transmitted block in the pre- and post-systems, i.e., $\mathrm{E}[\|\rho\mathbf{W}_{KM}^H\boldsymbol{\Theta}\mathbf{W}_{KM}\mathbf{U}\mathbf{s}\|^2] = \mathrm{E}[\|\mathbf{s}\|^2]$. Assuming $\mathrm{E}[\mathbf{s}\mathbf{s}^H] = \sigma_s^2\mathbf{I}_M$, we have $\rho = \sqrt{KM}\mathrm{tr}\{\boldsymbol{\Theta}\boldsymbol{\Theta}^H\}^{-\frac{1}{2}}$.

3.2 Weights of Pre-FDE/DC

3.2.1 ZF Pre-FDE/DC Weights

Here we derive the ZF weights for the pre-FDE/DC in the same way as in Sect. 2.3.1. The ZF condition is the same as (9) and the cost function is given by,

$$\begin{aligned} \mathrm{E}[||\mathbf{e}||^2] &= \mathrm{E}\left[\mathrm{tr}\left\{\left(\frac{1}{\rho}\mathbf{U}^{\mathrm{H}}\mathbf{n}\right)\left(\frac{1}{\rho}\mathbf{U}^{\mathrm{H}}\mathbf{n}\right)^{\mathrm{H}}\right\}\right], \\ &= \frac{\sigma_n^2 M}{\rho^2} = \frac{\sigma_n^2}{K}\mathrm{tr}\{\mathbf{\Theta}\mathbf{\Theta}^*\}. \end{aligned} \tag{23}$$

By minimizing (23) under the constraint (9), the optimum ZF weights of the pre-FDE/DC is derived as

$$\theta(m) = \frac{K\lambda(m)^*}{\sum_{i=0}^{K-1}|\lambda(iM+l)|^2}. \tag{24}$$
$$(l := m \pmod M), \quad m = 0, \cdots, KM-1)$$

3.2.2 MMSE Pre-FDE/DC Weights

Next, we derive the MMSE weights of the pre-FDE/DC. The MSE is represented by

$$\begin{aligned} \mathrm{MSE} = \mathrm{tr}\{&\sigma_s^2\mathbf{I}_M \\ &+ \sigma_s^2\mathbf{U}^H\mathbf{W}_{KM}^H\mathbf{\Lambda}\mathbf{\Theta}\mathbf{W}_{KM}\mathbf{U}\mathbf{U}^H\mathbf{W}_{KM}^H\mathbf{\Theta}^*\mathbf{\Lambda}^*\mathbf{W}_{KM}\mathbf{U} \\ &+ \frac{\sigma_n^2}{\rho^2}\mathbf{I}_M - \sigma_s^2\mathbf{U}^H\mathbf{W}_{KM}\mathbf{\Theta}^*\mathbf{\Lambda}^*\mathbf{W}_{KM}\mathbf{U} \\ &- \sigma_s^2\mathbf{U}^H\mathbf{W}_{KM}^H\mathbf{\Lambda}\mathbf{\Theta}\mathbf{W}_{KM}\mathbf{U}\}. \end{aligned} \tag{25}$$

The optimum $\mathbf{\Theta}$ satisfies $\partial(\mathrm{MSE})/\partial\mathbf{\Theta}^H = \mathbf{0}_{KM\times M}$, i.e.,

$$\begin{aligned} &\sigma_s^2\mathbf{W}_{KM}^H\mathbf{\Lambda}^*\mathbf{W}_{KM}\mathbf{U}\mathbf{U}^H\mathbf{W}_{KM}^H\mathbf{\Lambda}\mathbf{\Theta}\mathbf{W}_{KM}\mathbf{U} \\ &\quad + \sigma_n^2\mathbf{W}_{KM}^H\mathbf{\Theta}\mathbf{W}_{KM}\mathbf{U} - \sigma_s^2\mathbf{W}_{KM}^H\mathbf{\Lambda}^*\mathbf{W}_{KM}\mathbf{U} = \mathbf{0}_{KM\times M}. \end{aligned} \tag{26}$$

Thus we have

$$\theta(m) = \frac{K\lambda(m)^*}{\sum_{i=0}^{K-1}|\lambda(iM+l)|^2 + \frac{K\sigma_n^2}{\sigma_s^2}}. \tag{27}$$
$$(l := m \pmod M), \quad m = 0, \cdots, KM-1)$$

It should be mentioned that, since the pre-FDE/DC has no effect on the noise $\mathbf{n}$, the colored noise problem as in the post-FDE/DC case does not occur.

4. Proposed Pre- and Post-Equalization and Diversity Combining Method for OFDM Scheme

So far, we have discussed post-equalization and diversity combining method for SC-CP scheme depicted in Fig. 5(a). However, OFDM is also an significant block transmission scheme with the CP. Since the SC-CP scheme and the OFDM scheme differ only in the placement of an IDFT [4], we have the block diagram of the proposed OFDM scheme with the FDE/DC depicted in Fig. 5(b) by substituting $\mathbf{W}_M^H\mathbf{s}$ for $\mathbf{s}$ and $\mathbf{W}_M\hat{\mathbf{s}}$ for $\hat{\mathbf{s}}$ in Fig. 5(a). Moreover, both $\mathbf{W}_M^H$ and $\mathbf{W}_M$ are unitary matrices, thus the placement of inverse IFFT have no effect on the cost functions Eqs. (13), (15), (23) and (25). For example, the MSE for the proposed OFDM scheme with the FDE/DC is given by,

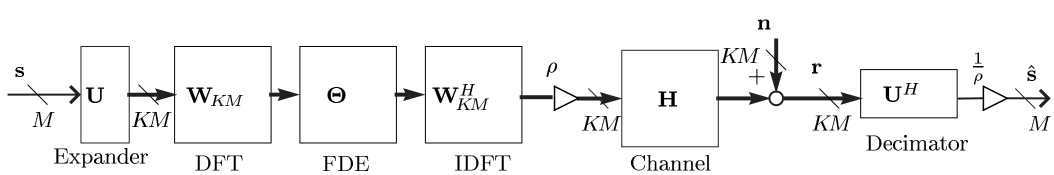

Fig. 4 The block diagram of SC-CP scheme with the pre-FDE/DC.

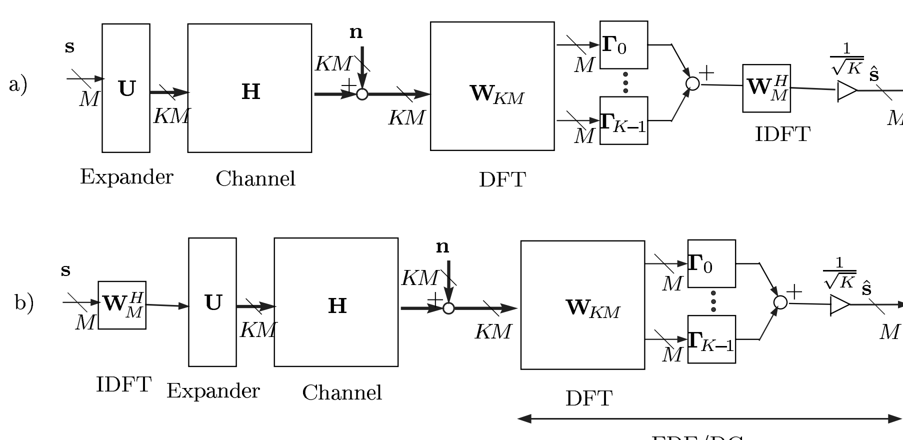

Fig. 5 The block diagram of (a) SC-CP and (b) OFDM scheme with the FDE/DC.

$$\begin{aligned}\mathrm{MSE_{OFDM}} &= \mathrm{E}[||\mathbf{s}_{\mathrm{OFDM}} - \hat{\mathbf{s}}_{\mathrm{OFDM}}||^2] \\ &= \mathrm{E}[||\mathbf{W}_M^H\mathbf{s} - \mathbf{W}_M^H\hat{\mathbf{s}}||^2] \\ &= \mathrm{E}[||\mathbf{s} - \hat{\mathbf{s}}||^2], \end{aligned} \tag{28}$$

where $\mathbf{s}_{\mathrm{OFDM}}$ and $\hat{\mathbf{s}}_{\mathrm{OFDM}}$ represent the information signal and FDE/DC output in the OFDM scheme, and $\mathbf{s}$ and $\hat{\mathbf{s}}$ are those of SC-CP scheme, respectively. Therefore, we can utilize the same FDE/DC weights as the SC-CP scheme for the OFDM scheme.

On the other hand, we can also adopt the proposed pre-equalization and diversity combining method to the OFDM scheme in the same manner and the same pre-FDE/DC weights as the SC-CP scheme can be used for the proposed OFDM scheme with the pre-FDE/DC.

5. Computer Simulations

Here we evaluate the BER performance and the PAPR of the transmitted signal via computer simulations. System parameters used in the simulations are summarized in Table 1. We have employed QPSK scheme with coherent detection for the modulation/demodulation scheme, and set the block size as $M = 256$ and the CP length as $N = 32$. The Tx and the Rx filters are assumed to be square-root raised-cosine filters with the roll-off factor $\alpha = 0.5$. We considered 10-path Rayleigh fading channels with an exponentially decaying power profile. We set the total channel order $L = 30$ and the whole response of the channel including the Tx and Rx filters is assumed to be known to the receiver. In our simulations, the BER performances of the proposed system are compared under the constraint of the same transmit energy per bit to the noise power density (E_b/N_0), e.g., in the cases of post-FDE/DC with QPSK modulation,

$$\frac{E_b}{N_0} = \frac{M}{M+N}\frac{\mathrm{E}[||\mathbf{s}||^2]}{2M\sigma_n}. \tag{29}$$

In pre-FDE/DC cases, thanks to the constant ρ, E_b/N_0 of the transmitted signal is the same as that of the post-FDE/DC cases.

5.1 BER Performance

First, we evaluate the BER performance of the FSE. Recalling that, the FSE is one special case of the proposed system with the FDE/DC. In this case, since $K \geq P = 1$, the colored noise problem occurs. Figures 6 and 7 show BER performances of the SC-CP and OFDM schemes with the FSE ($K = 2, 4$) and conventional symbol spaced equalizer (SSE) ($K = 1$) system versus E_b/N_0. From the figures, we can see that the FSE can improve the performance compared with the SSE in both schemes. However, there is no difference in performance between $K = 2$ and 4. This is because the transmitted signal bandwidth is limited by Tx and Rx filters up to $3/2$ times greater than the symbol rate and $K = 2$ is enough to perfectly observe the received signal. When $K = 2$ or 4, oversampling yields the colored noise due to the Rx filter, and the proposed MMSE-FDE/DC can not be the optimal linear MMSE equalizer and combiner. However, the figures show that the MMSE-FDE/DC can achieve almost the optimal performance for both schemes.

Figures 8 and 9 show the BER performances of the SC-CP and OFDM schemes with the FDE/DC ($K = P = 2, 4$) and conventional methods ($K = P = 1$) versus E_b/N_0. Both in the SC-CP and OFDM schemes, we can see significant improvements in the BER performance due to the frequency

Table 1 System parameters.

Mod. /Demod. Scheme	QPSK
Block Size	$M = 256$
Length of CP	32
Tx and Rx filters	Square-Root Raised-Cosine Filter (Roll-Off Factor $\alpha = 0.5$)
Channel Model	Exponentially Decaying 10-path Rayleigh Fading Channels (Decaying Factor 0.5)
Channel Order	$L = 30$
Channel Noise	AWGN
Channel Estimation	Ideal

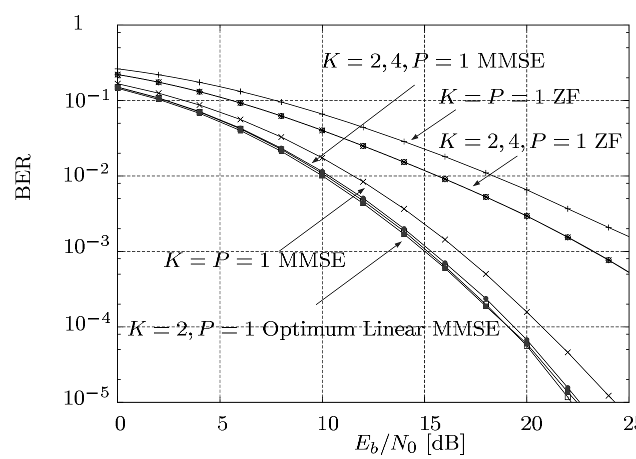

Fig. 6 The BER performance versus E_b/N_0 of uncoded SC-CP scheme with the FSE.

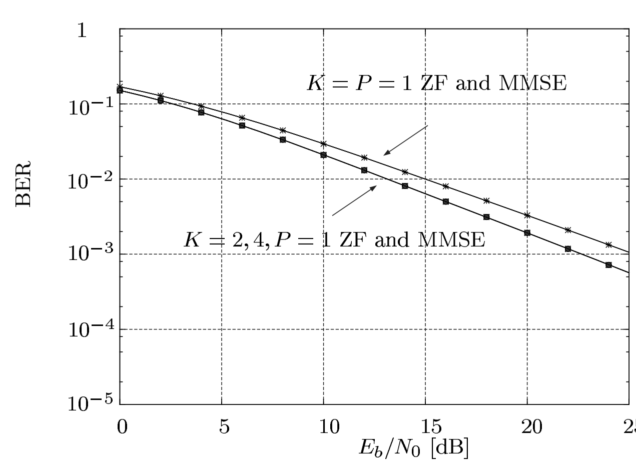

Fig. 7 The BER performance versus E_b/N_0 of uncoded OFDM scheme with the FSE.

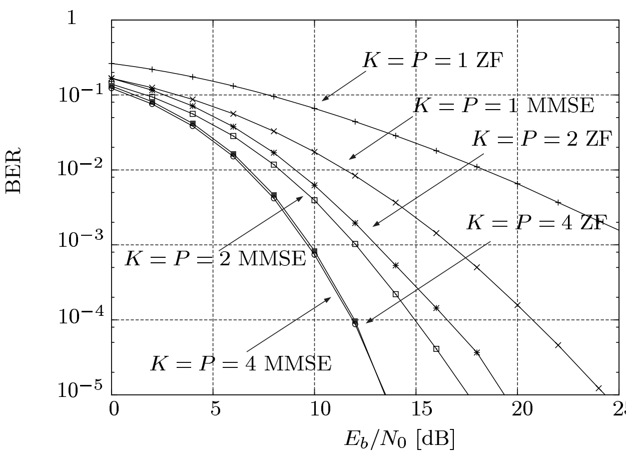

Fig. 8 The BER performance versus E_b/N_0 of uncoded SC-CP scheme with the FDE/DC.

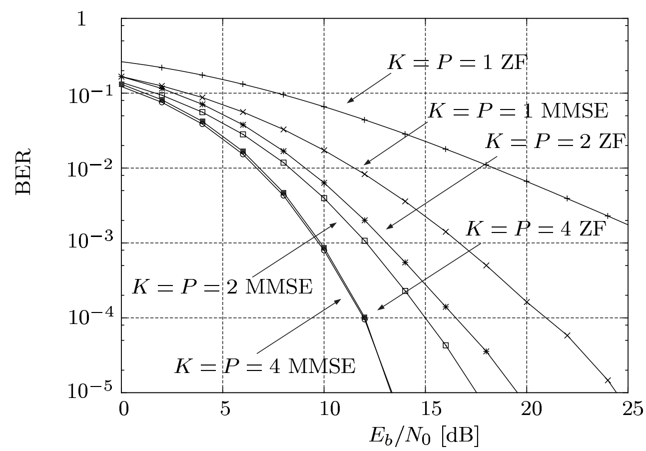

Fig. 10 The BER performance versus E_b/N_0 of uncoded SC-CP scheme with the pre-FDE/DC.

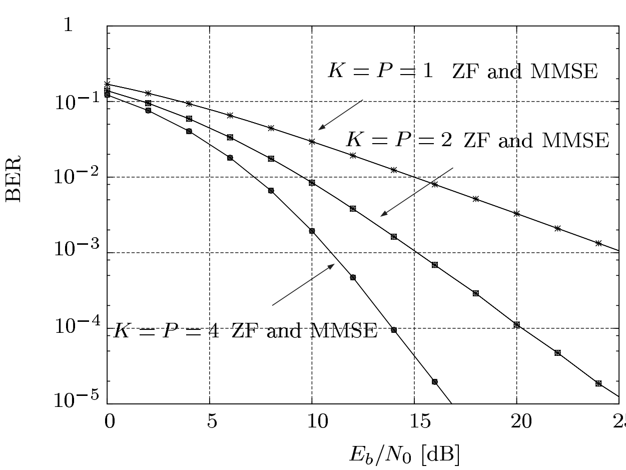

Fig. 9 The BER performance versus E_b/N_0 of uncoded OFDM scheme with the FDE/DC.

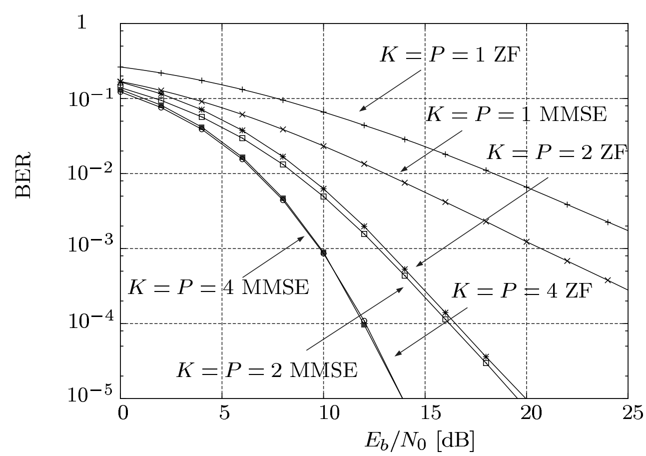

Fig. 11 The BER performance versus E_b/N_0 of uncoded OFDM scheme with the pre-FDE/DC.

diversity effect. This shows that the proposed method can efficiently provide diversity gain.

Figures 10 and 11 show the BER performances of the SC-CP and OFDM schemes with the pre-FDE/DC ($K = P = 2, 4$) and conventional methods ($K = P = 1$) versus E_b/N_0. From the figures, we can see that the proposed methods can achieve diversity combining and provide diversity gain with the simple receiver. In SC-CP case, the pre- and post-FDE/DC shows almost the same performance. On the other hand, in OFDM scheme, there is a performance difference between the pre- and post-FDE/DC. Especially, the difference is significant in the case of $K = P = 1$. We have analized this phenomenon in Appendix.

The BER performance of the proposed method in coded systems is our another interest. Figures 12 and 13 show the BER performances of the turbo coded SC-CP and OFDM schemes with the ZF and MMSE-FDE/DC ($K = P = 2, 4$) and conventional methods ($K = P = 1$) versus E_b/N_0, where the coding rate is 1/3, constraint length for turbo decoding is 4, and the maximum number of itera-

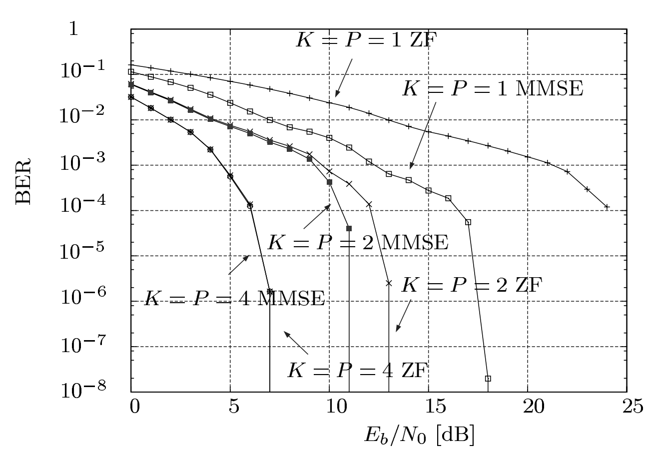

Fig. 12 The BER performance versus E_b/N_0 of turbo coded SC-CP scheme with the FDE/DC.

tion for turbo decoding is 8. From the figures, the proposed FDE/DC can also acheive superior performance due to the frequency diversity in coded systems.

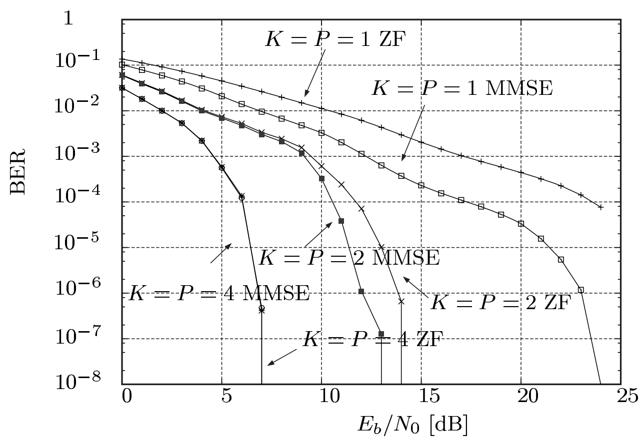

Fig. 13 The BER performance versus E_b/N_0 of turbo coded OFDM scheme with the FDE/DC.

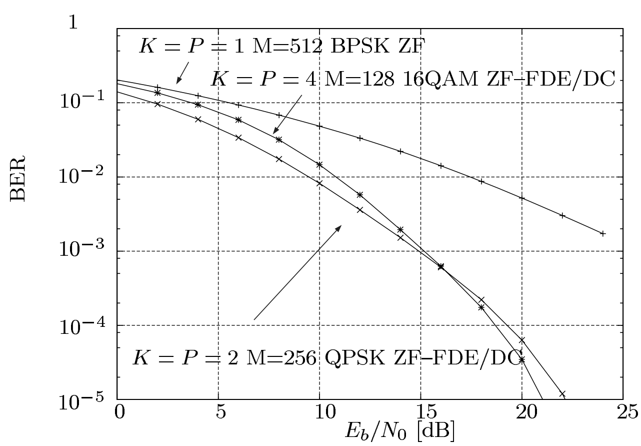

Fig. 14 The BER performance versus SNR of uncoded SC-CP scheme with the ZF-FDE/DC for a given transmission rate.

In the previous simulations, the transmission rate is changed for a different K and P, because we have take the proposed scheme to be one of possible option in adaptive modulation system. However, it is meaningful to compare the performances for a given transmission rate. Figure 14 is the simulation result where, under the constraint of the same transmit SNR, we set $M = 512$ with BPSK modulation for $K = P = 1$, $M = 256$ with QPSK modulation for $K = P = 2$ and $M = 128$ with 16QAM modulation for $K = P = 4$. From the figure, it is shown that the proposed scheme can improve the BER performance for a given frequency efficiency case.

5.2 PAPR of Transmitted Signal

Here we evaluate the PAPR of the transmitted signal. Figures 15 and 16 show the PAPR of the SC-CP and OFDM schemes with the proposed methods versus their complementary cumulative distribution functions (CCDF). The CCDF of the PAPR in conventional SC-CP and OFDM scheme are also plotted in the figures. From the figures, we can see that the PAPR of the transmitted signal increases

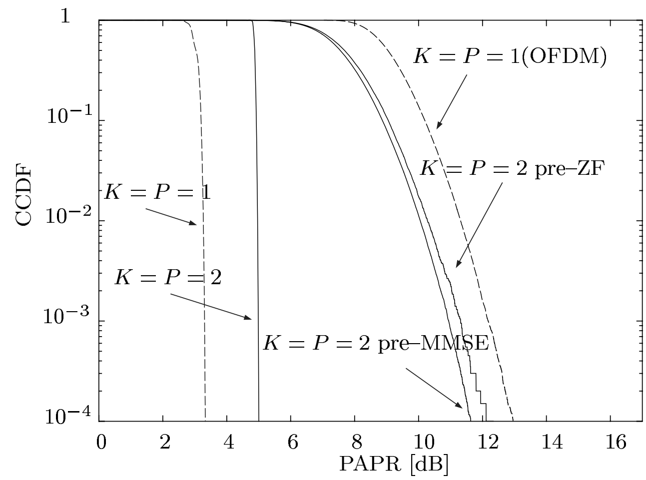

Fig. 15 The CCDF versus PAPR of SC-CP scheme with proposed diversity methods.

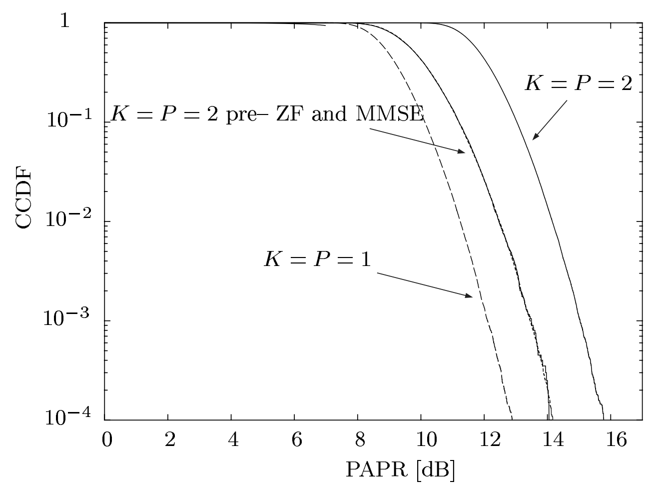

Fig. 16 The CCDF versus PAPR of OFDM scheme with proposed methods.

by using proposed methods. However the PAPR of SC-CP scheme with the post-FDE/DC is much smaller than that of conventional OFDM scheme. Moreover the PAPRs of SC-CP schemes with all the other proposed methods are still smaller than that of the conventional OFDM signal. On the contrary, the PAPR of OFDM scheme with pre-FDE/DC is much smaller than the post-FDE/DC case.

6. Conclusions

In this paper, we have proposed simple pre- and post-frequency domain equalization and diversity combining methods for block transmission with the CP. We have derived the equalizer and combiner weights based on the ZF and MMSE criteria. Moreover we have evaluated the performance of proposed methods via computer simulations. From all the results, it can be concluded that the proposed methods can achieve the diversity gain with slight increase in the complexity of configuration compared with the conventional FDE systems.

References

[1] A. Peled and A. Ruiz, "Frequency domain data transmission using reduced computational complexity algorithm," Proc. ICASSP, pp.964–967, April 1980.
[2] L.J. Cimini, Jr., "Analysis and simulation of a digital mobile channel using orthogonal frequency division multiplexing," IEEE Trans. Commun., vol.COM-33, no.7, pp.529–540, July 1985.
[3] J.A.C. Bingham, "Multicarirrer modulation for data transmission: An idea whose time has come," IEEE Commun. Mag., vol.28, no.5, pp.5–14, May 1990.
[4] D. Falconer, S.L. Ariyavisitakul, A.B. Seeyar, and B. Edison, "Frequency domain eualization for single-carrier broadband wireless systems," IEEE Commun. Mag., vol.40, no.4, pp.58–66, Feb. 2002.
[5] J.G. Proakis, Digital Communications, 3rd ed., pp.617–621, McGraw-Hill, 1995.
[6] P.P. Vaidyanathan and B. Vrcelj, "Theory of fractionally spaced cyclic-prefix equalizers," Proc. ICASSP, vol.2, pp.1277–1280, May 2002.
[7] C. Tepedelenlioglu and R. Challagulla, "Low-complexity multipath diversity thorough fractional sampling in OFDM," IEEE Trans. Signal Process., vol.52, no.11, pp.3104–3116, Nov. 2004.
[8] R.M. Gray, "Toeplitz and circulant matrices: A review," http://ee.stanford.edu/gray/toeplitz.pdf, 2002.
[9] P.P. Vaidyanathan, "Multirate digital filters, filter banks, polyphase networks, and applications: A tutorial," Proc. IEEE, vol.78, pp.56–92, Jan. 1990.
[10] G.H. Golub and C.F. van Loan, Matrix Computations, 3rd ed., Johns Hopkins Univ. Press, Baltimore, MD, 1996.
[11] Y. Yoshida, K. Hayashi, and H. Sakai, "Fractionally spaced equalization and frequency diversity methods for block transmission with cyclic prefix," Proc. 2nd IEEE VTS Asia Pacific Wireless Communications Symposium (APWCS2005), pp.110–114, Aug. 2005.

Appendix: BER Analysis of OFDM Scheme with Pre- and Post-FDE

In our simulation in Sect. 5, unlike the SC-CP scheme, there is a difference between the BER performance of the OFDM scheme with pre- and post-FDE/DC. The difference is especially significant in the case of $K = P = 1$. Therefore, for simplicity, we consider the conventional OFDM scheme with post-FDE and pre-FDE, where QPSK modulation. In the post-FDE case, the equalizer output of the l-th subcarrier ($l = 1, 2, \cdots, M$)is can be represented as

$$\hat{s}_l = \gamma_l \lambda_l s_l + \gamma_l n_l. \tag{A· 1}$$

Here s_l denotes the transmitted symbol of the l-th subcarrier, λ_l frequency response of the channel corresponding to the l-th subcarrier, γ_l denotes the equalizer weights and n_l is additive Gaussian noise (AWGN) component in discrete frequency domain.

In OFDM scheme, each subcarrier is assumed to pass through the flat fading channel and AWGN, BER performance can be given by averaging the BER of each subcarrier. Signal to noise power ratio (SNR) of the l-th subcarrier at the equalizer output is represented as,

$$\mathrm{SNR}_{\mathrm{post}} = \frac{2|\lambda_l|^2 E_b}{N_0}, \tag{A· 2}$$

where E_b denotes transmitted energy per information bit and N_0 is the variance of the noise. From [5], the BER of the l-th subcarrier can be approximated as

$$P_l \sim 2Q\left(\sqrt{\frac{4|\lambda_l|^2 E_b}{N_0}}\sin\frac{\pi}{4}\right). \tag{A· 3}$$

Here,

$$Q(x) = \frac{1}{\sqrt{2}}\int_x^{\infty} \exp^{-t^2/2}\, dt. \tag{A· 4}$$

As a result, the BER of the OFDM scheme with post-FDE is given by

$$P_{\mathrm{post}} \sim \frac{1}{M}\sum_{l=1}^{M} 2Q\left(\sqrt{\frac{4|\lambda_l|^2 E_b}{N_0}}\sin\frac{\pi}{4}\right). \tag{A· 5}$$

It is clear from the equation that, since the choice of the weights γ does not effect on BER performance, both ZF and MMSE weights shows the same BER performance.

On the other hand, OFDM scheme with pre-FDE case, the detector input signal of the l-th subcarrier can be represented as

$$\hat{s}_l = \rho^{\frac{1}{2}} \lambda_l \theta_l s_l + n_l, \tag{A· 6}$$

where θ_l is the pre-FDE weight corresponding to the l-th subcarrier and,

$$\rho = \frac{M}{\sum_{l=1}^{M} |\theta_l|^2}. \tag{A· 7}$$

Therefore the SNR of detector input corresponding to the l-th subcarrier is

$$\mathrm{SNR}_{\mathrm{pre}} = \frac{2\rho|\lambda_l|^2|\theta_l|^2 E_b}{N_0}. \tag{A· 8}$$

It should be mentioned that E_b is defined as the total transmitted energy per bit and it is the same as the post-FDE case, meanwhile the allocated transmitted power at the l-th subcarrier is $2\rho|\theta_l|^2 E_b$. The BER performance of OFDM scheme with pre-FDE is given by

$$P_{\mathrm{pre}} \sim \frac{1}{M}\sum_{l=1}^{M} 2Q\left(\sqrt{\frac{4\rho|\lambda_l|^2|\theta_l|^2 E_b}{N_0}}\sin\frac{\pi}{4}\right). \tag{A· 9}$$

As a result, unlike the post-FDE case, the BER of the pre-FDE depends on the choice of equalizer weights.

Yuki Yoshida received the B.E. and M. Info. degrees in Systems Science from Kyoto University, Kyoto, Japan, in 2004 and 2005, respectively. He is currently working towards a Ph.D. in the Department of Systems Science, Graduate School of Informatics, Kyoto University.

Kazunori Hayashi received the B.E., M.E. and Ph.D. degrees in communication engineering from Osaka University, Osaka, Japan, in 1997, 1999 and 2002, respectively. Since 2002, he has been with the Department of System Science Graduate School of Informatics, Kyoto University. He is currently an Assistant Professor there. His research interest include digital signal processing for communications systems.

Hideaki Sakai received the B.E. and D.E. degrees in applied mathmatics and physics from Kyoto University, Kyoto, Japan, in 1972 and 1981, respectively. From 1975 to 1978, he was with Tokushima University. He is currently a Professor in the Department of Systems Science, Graduate School of Informatics, Kyoto University. He spent six months from 1987 to 1988 at Stanford University as a Visiting Scholar. His research interests are in the areas of adaptive and statistical signal processing. He served as an associated editor of IEEE Trans. Signal Processing from Jan. 1999 to Jan. 2001 and an IEEE Fellow from 2007.